Diffusion and dynamical heterogeneity in simulated liquid SiO_2 under high pressure

2007 J. Phys.: Condens. Matter 19 116104

(http://iopscience.iop.org/0953-8984/19/11/116104)

IOP PUBLISHING JOURNAL OF PHYSICS: CONDENSED MATTER

J. Phys.: Condens. Matter **19** (2007) 116104 (14pp) doi:10.1088/0953-8984/19/11/116104

Diffusion and dynamical heterogeneity in simulated liquid SiO_2 under high pressure

Vo Van Hoang[1], Hoang Zung[2] and Nguyen Trung Hai[3]

[1] Department of Physics, Institute of Technology, HCM City National University, 268 Ly Thuong Kiet Street, District 10, HochiMinh City, Vietnam
[2] Department of Science and Technology, National University of HochiMinh City, Vietnam
[3] Department of Physics, College of Natural Science, HCM City National University, Vietnam

E-mail: vvhoang2002@yahoo.com

Received 30 September 2006, in final form 18 January 2007
Published 27 February 2007
Online at stacks.iop.org/JPhysCM/19/116104

Abstract

Diffusion of Si and O ions in simulated liquid SiO_2 under high pressure (or high density) have been studied in a model containing 3000 ions under periodic boundary conditions with pairwise interatomic potentials which have a weak electrostatic interaction and Morse-type short-range interaction. In order to observe diffusion in the liquid state, amorphous models at fixed densities of 2.20, 4.30 and 5.35 g cm^{-3} have been heated up from 350 to 7000 K via molecular dynamics (MD) simulation and the diffusion constant has been calculated at temperatures ranging from above the melting point to 7000 K. Calculations show that the temperature dependence of the diffusion constant D of components in the system shows an Arrhenius law at relatively low temperatures above the melting point and shows a power law, $D \propto (T - T_C)^\gamma$, at higher temperatures. Dynamical heterogeneities under high pressure have been observed and discussed.

1. Introduction

Diffusion of ions in liquid SiO_2 has attracted great interest and has been under intensive investigation by both experiment and computer simulation for the past three decades. The diffusion constant of Si^{4+} and O^{2-} ions in simulated liquid SiO_2 at ambient pressure has been calculated via MD simulation using Born–Mayer–Huggins interatomic potentials by Woodcock *et al*, and has a value of around $(5.0 \pm 0.5) \times 10^{-5}$ cm^2 s^{-1} and was of the order of magnitude predicted from viscosity extrapolation [1]. It was found experimentally that the activation energies for the diffusion of Si and O in silica are equal to 6 and 4.7 eV, respectively [2, 3]. However, more details about diffusion in liquid SiO_2 with the BKS interatomic potentials were obtained later by Horbach *et al* [4]. It was found that the temperature dependence of the diffusion constant D shows an Arrhenius law at low temperatures with an activation energy

that is very close to the experimental data in [2, 3], and this dependence shows a power law, $D \propto (T - T_C)^\gamma$, at higher temperatures, as predicted by mode coupling theory (MCT). The critical temperature has the value $T_c = 3330$ K, and the exponent γ is close to 2.10 (see more details in [4]). A power law behaviour for the dynamics in other tetrahedral network structure liquids such as GeO_2 or H_2O has also been found. The temperature dependence of the diffusion constant in water has been observed by both experiment and computer simulation. Measurements of the self-diffusion constant in supercooled water under high pressure up to 300 MPa have been reported where the temperature dependence of the self-diffusion constant in H_2O showed a power law, $D = D_0 T^{1/2}(T/T_s - 1)^\gamma$, with the value for γ ranging from 1.80 to 2.46 [5]. The power law behaviour of the dynamics in water has been tested later by MD simulation. Starr *et al* calculated the isochores of the diffusion constant in water over a wide temperature range at densities ranging from 0.95 to 1.40 g cm^{-3} using the extended simple point-charge potential [6]. Also, at each density studied, they found a good fitting of a power law: $D \sim (T/T_c - 1)^\gamma$. Moreover, they found that γ decreases under pressure for their model whereas it increases experimentally [6] and, as suggested, this disagreement indicated the need to improve the dynamic properties of water models. Similar simulation results for water at temperatures from 350 K down to 190 K and at pressures from 2.5 GPa down to −300 MPa also confirmed the prediction of MCT for the dynamics of weakly supercooled liquids, i.e. the calculated data of each isochore showed a power law: $D \sim (T/T_c - 1)^\gamma$ (see in [7]). Power law behaviour for diffusion in liquid simulated GeO_2 at ambient pressure has been observed [8]. However, a possible appearance of the power law behaviour for diffusion in liquid silica under high pressure has not been tested yet. Therefore, clarification of this problem is our main aim here in the present work. In addition, we also present results for dynamical heterogeneity in liquid silica under high pressure.

2. Calculation

It is important to choose appropriate interatomic potentials for the system to be simulated. The results of numerous experimental studies of oxide systems indicate a substantial contribution of ionic bonding to interatomic interactions due to the high electronegativity of the oxygen atoms [9]. On the other hand, the covalent interaction is also an important part of the system. In the simulation of oxides, the covalent interaction is described in terms of three-particle potentials, which significantly increase the computation time. Since ionic contribution cannot be neglected for oxides, the Coulomb interactions have to be considered. Further, simulation of oxides with mixed ion and covalent bonding requires too many force parameters, and is very difficult to carry out. Therefore, the models have to be simplified and the choice of a model based on ionic interactions has significant advantages. The results of simulations of oxides using the ionic model over the past three decades has confirmed this choice (see [1, 4, 8, 9] and references therein). Concerning the silica system, various kinds of potentials are used for different purposes. Woodcock *et al* [1] used a Born–Mayer–Huggins (BMH) potential which was originally proposed for describing the interaction between ions based on full charges, and generally it gives elastic moduli that are significantly larger than the experimental values. Later, pairwise additive models such as TTAM [10, 11] and BKS [12] potentials used fractional charges, which significantly improved the accuracy of these models in terms of reproducing the structure and properties of SiO_2. The optimization of these potential parameters was based on *ab initio* calculations of small clusters, and it seems that both potentials overestimate the inter-tetrahedral angle, indicating that the Si–O–Si bending interaction is too weak [13]. Moreover, via a comparison of the melting temperature and the density profile at high temperatures predicted by potentials in the literature for SiO_2, it was found that the high-temperature

behaviour was best described by the potentials with weak long-range interactions and a Morse-type potential for short-range interactions [14], as given below:

$$U_{ij}(r) = \frac{q_i q_j}{r} + D_0\left\{\exp\left[\gamma\left(1 - \frac{r}{R_0}\right)\right] - 2\exp\left[\frac{1}{2}\gamma\left(1 - \frac{r}{R_0}\right)\right]\right\} \tag{1}$$

where q_i and q_j represent the charges of atoms i and j—for Si atoms $q_{\mathrm{Si}} = +1.30e$ and for O atoms $q_{\mathrm{O}} = -0.65e$ (where e is the elementary charge unit); r denotes the interatomic distance between atoms i and j; and D_0, γ and R_0 are the parameters of the Morse potentials representing the short-range interactions in the system.

The Morse potential parameters for the silica system can be found in [14–16]. These potentials have been used successfully for MD simulation of both the structure and thermodynamic properties of silica [14–16], in particular for an investigation of the structure changes in cristobalite and silica glass at high temperatures [15]. These potentials reproduced well the melting temperature of cristobalite and the glass phase transition temperature of silica glass, and the calculated data were more accurate than those observed in other simulation works in which traditional interatomic potentials with stronger electrostatic interaction have been used, such as the TTAM or BKS potentials [10–12]. Moreover, the calculated results in [15] reproduced the density maxima at around 1800 K for cristobalite and 1700 K for silica glass, which are very close to the experimental data. The potential (1) was originally proposed with the charge equilibrium scheme and was then slightly modified into a potential with the fixed charges $q_{\mathrm{Si}} = +1.30e$ for Si atom and $q_{\mathrm{O}} = -0.65e$ for O atom (see more details in [15]). Also, therefore, such interatomic potentials have been used again here. We use the Verlet algorithm with an MD time step of 1.60 fs. Initial well-relaxed amorphous SiO_2 models at 350 K and at the three different densities of 2.2, 4.30 and 5.35 g cm^{-3} have previously been obtained in [16]. The three models have been heated up to 7000 K at fixed density (i.e. an isochore process) at a heating rate of 4.2945×10^{12} K s^{-1}. The model obtained at each temperature above the melting point has been relaxed for 100 000 MD steps (or 160 ps) in order to calculate the diffusion constant and static properties. In order to calculate coordination number distributions in SiO_2 models, we adopt the fixed values $R_{\mathrm{Si-Si}} = 3.30$ Å, $R_{\mathrm{Si-O}} = 2.10$ Å and $R_{\mathrm{O-O}} = 3.00$ Å. Here R denotes a cutoff radius, which is chosen to be the position of the minimum after the first peak in the radial distribution function (PRDF), $g_{ij}(r)$, for the amorphous state at the temperature of 350 K and at 2.20 g cm^{-3}.

3. Results and discussions

Diffusion has been studied only at temperatures above the melting point; therefore, it is necessary to determine the melting temperature for the system at each density presented above. The melting temperature T_{m} is determined from the intersection of a linear high- and low-temperature extrapolation of the potential energy, U (see figure 1). The values of T_{m} are equal to 2260, 2480 and 2899 K for the models at 2.20, 4.30 and 5.35 g cm^{-3}. This means that T_{m} depends strongly on the density of the system. Moreover, our calculated T_{m} for a model at the ambient pressure density 2.20 g cm^{-3} is higher than those obtained in practice (i.e. $T_{\mathrm{m}} = 1986$ K [17]). The discrepancy may be related to the extremely high simulation heating rate compared with those used in practice, and the model size is rather small. Moreover, it also indicates that the interatomic potentials used in the present work do not describe the melting point for amorphous silica well.

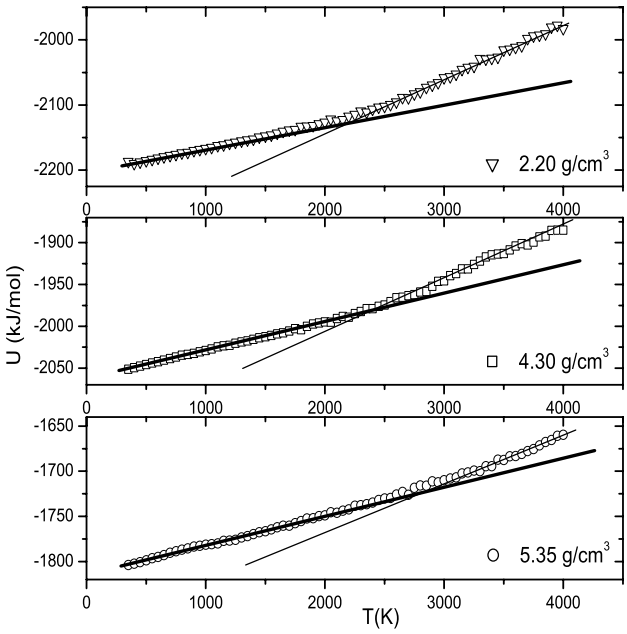

Figure 1. Temperature dependence of potential energy, U, of the system.

Table 1. Structural characteristics of liquid SiO_2 at three different densities upon heating from 3000 to 7000 K: r_{ij}—mean interatomic distance or positions of the first peaks in PRDFs; Z_{ij}—the average coordination number.

		r_{ij} (Å)			Z_{ij}			
Density (g cm^{-3})	T (K)	Si–Si	Si–O	O–O	Si–Si	Si–O	O–Si	O–O
2.20	3000	3.04	1.53	2.57	2.92	3.80	1.90	5.38
	5000	3.01	1.52	2.59	2.56	3.37	1.68	4.79
	7000	3.00	1.51	2.60	2.46	3.13	1.56	4.54
4.30	3000	2.89	1.55	2.31	7.31	5.07	2.54	10.83
	5000	2.85	1.53	2.27	6.96	4.88	2.44	10.36
	7000	2.82	1.53	2.24	6.74	4.73	2.36	10.11
5.35	3000	2.74	1.54	2.14	9.95	6.00	3.00	12.23
	5000	2.72	1.53	2.11	9.63	5.94	2.97	12.15
	7000	2.69	1.52	2.09	9.28	5.81	2.90	11.99

3.1. Diffusion

Before discussing diffusion in the system under high pressure, we would like to turn out our attention to the changes in structure of the system upon heating from 3000 to 7000 K. As shown in table 1, at 3000 K the models at three different densities of 2.20, 4.30 and 5.35 g cm^{-3} have tetrahedral, pentahedral and octahedral network structures, respectively (i.e. the mean coordination number for the Si–O pair, $Z_{\mathrm{Si-O}}$, is equal to 3.80, 5.07 and 6.00, respectively) although models at 2.20 g cm^{-3} have a weak tetrahedrality. Also, upon heating, the structure of a model changes significantly. The mean interatomic distance and the coordination number for all atomic pairs decrease with temperature (see table 1). However, the Si–O interatomic

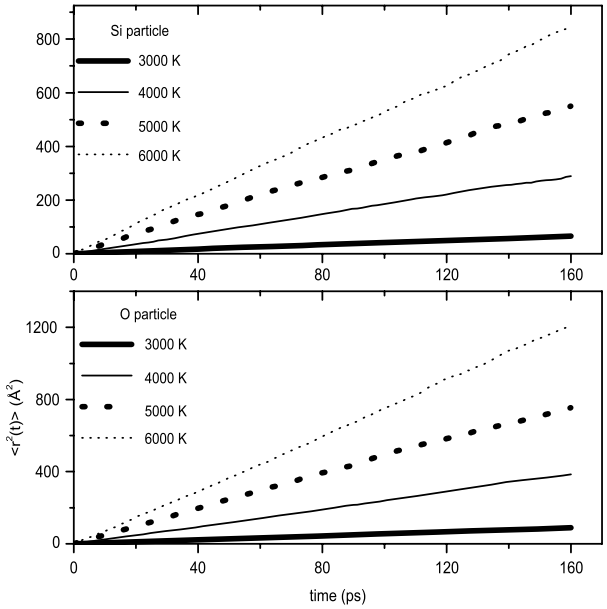

Figure 2. Mean-squared atomic displacement, $\langle r^2(t)\rangle$, of Si and O particles in liquid SiO_2 models obtained at different temperatures and at a density of 4.30 g cm^{-3}.

distance remains almost unaffected over the range of temperatures between 3000 and 7000 K due to the strong interaction between $Si^{1.30+}$ and $O^{0.65-}$ ions. The following points can be mentioned: the tetrahedrality of the model at 2.20 g cm^{-3} breaks upon heating and, at high temperatures, it transforms into a phase with $Z_{Si-O} \approx 3.00$. In contrast, although significant changes in structure have been found in models at higher densities of 4.30 and 5.35 g cm^{-3}, upon heating one can see that the main structural units remain dominant in the system (i.e. SiO_5 in models at 4.30 g cm^{-3} and SiO_6 in models at 5.35 g cm^{-3}). In other words, pentahedrality and octahedrality remain in the models at 4.30 and 5.35 g cm^{-3} upon heating from 3000 to 7000 K. However, it is well known that even small changes in the structure can cause dramatic changes in the dynamics of the system, and one can see this via the changes in diffusion and dynamical heterogeneities in the system below when the temperature increases. Overall, small changes in the mean interatomic distances for the models at three different densities over a wide temperature range from 3000 to 7000 K are related to the low thermal expansion coefficient of silica (see table 1).

One can determine the diffusion constant of particles in the system via the Einstein relation, $\lim_{t\to\infty} \frac{\langle r^2(t)\rangle}{6t} = D$, where $\langle r^2(t)\rangle$ is the mean-squared atomic displacement (figure 2) and the diffusion constant with error bars at different temperatures has been presented in table 2. The diffusion of atomic species has been studied in the liquid state of the system (at temperatures above the melting point), i.e. at temperatures ranging from 2500 to 7000 K for models at 2.20 g cm^{-3}, from 2750 to 7000 K for models at 4.30 g cm^{-3}, and from 3000 to 7000 K for models at 5.35 g cm^{-3}. As shown in figure 3, the diffusion constant ratio, $\frac{D_O}{D_{Si}}$, is greater than unity for the temperature range studied, and this means that the oxygen mobility is always larger than that for silicon. For models at a density $\rho \leqslant 4.30$ g cm^{-3}, the ratio is nearly constant for the whole temperature range, indicating the intimate connection between the diffusion of Si and O ions to each other. In contrast, the curve for the system at 5.35 g cm^{-3} strongly deviates from the first two curves presented, which is clear evidence of the changes in the diffusion

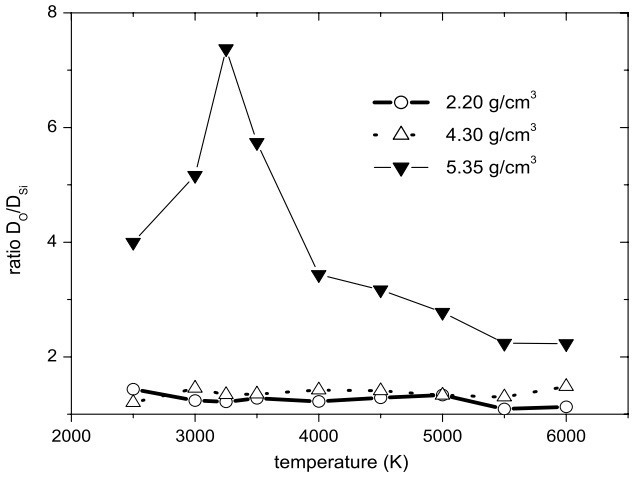

Figure 3. Temperature dependence of the ratio of diffusion constants of Si and O particles, $\frac{D_O}{D_{Si}}$, in liquid SiO_2.

Table 2. Diffusion constant, D in 10^{-6} cm^2 s^{-1}, of atomic species in liquid SiO_2 models at three different densities.

	2.20 g cm^{-3}		4.30 g cm^{-3}		5.35 g cm^{-3}	
T (K)	D_{Si}	D_O	D_{Si}	D_O	D_{Si}	D_O
2500	2.35 ± 0.03	3.37 ± 0.03	—	—	—	—
2750	8.25 ± 0.08	10.59 ± 0.09	2.88 ± 0.02	4.18 ± 0.03	—	—
3000	20.26 ± 0.20	25.14 ± 0.11	6.38 ± 0.04	9.26 ± 0.06	0.06 ± 0.003	0.31 ± 0.006
3250	34.50 ± 0.82	42.00 ± 0.71	11.18 ± 0.11	15.00 ± 0.05	0.16 ± 0.010	1.18 ± 0.03
3500	54.12 ± 0.95	69.15 ± 0.80	15.98 ± 0.13	21.58 ± 0.20	0.50 ± 0.007	2.87 ± 0.02
4000	108.70 ± 1.09	132.98 ± 0.87	29.11 ± 0.16	41.38 ± 0.21	2.45 ± 0.02	8.42 ± 0.03
4500	168.90 ± 1.30	217.20 ± 1.12	44.82 ± 0.22	63.14 ± 0.25	5.79 ± 0.05	18.34 ± 0.08
5000	203.60 ± 1.53	271.70 ± 1.05	55.97 ± 0.36	74.38 ± 0.38	10.64 ± 0.06	29.55 ± 0.14
5500	313.00 ± 2.21	341.60 ± 1.57	75.95 ± 0.40	98.77 ± 0.41	18.31 ± 0.09	41.00 ± 0.15
6000	373.00 ± 1.12	421.10 ± 1.42	87.33 ± 0.42	129.60 ± 0.42	26.00 ± 0.08	58.00 ± 0.25
6500	435.74 ± 2.42	498.57 ± 0.93	118.72 ± 0.35	158.60 ± 0.54	33.48 ± 0.19	73.64 ± 0.23
7000	474.89 ± 3.00	576.32 ± 1.48	133.81 ± 0.44	171.10 ± 0.69	41.19 ± 0.17	90.06 ± 0.56

mechanism of ions in an octahedral network structure, i.e. the non-connected diffusion of Si and O ions dominates in the system. According to our calculations, there are significant amounts of SiO_5 and SiO_7 units, in addition to the main structural units SiO_6, in models at 5.35 g cm^{-3}, and the fraction of Si atoms with other coordinations is very small (table 3). As the temperature increases, the fraction of dominant SiO_6 units in the octahedral network structure decreases, while the fraction of structural defects (i.e. SiO_5 and SiO_7) in the system increases. Therefore, it can be suggested that the diffusion of oxygen ions in this phase mainly takes place by breaking the Si–O bonds of SiO_6 sites, i.e. it leads to the formation of SiO_5 defects and non-bonding oxygen ions, and then the latter attach to other SiO_6 sites to form overcoordinated SiO_7 defects. In contrast, Si ions are located in the centre of SiO_x polyhedra and their diffusion mechanism almost does not change in the models at three different densities. Such a situation leads to the occurrence of the non-connected diffusion of Si and O ions. Temperature-induced network-breaking defects can be represented by the following reaction: $2SiO_6 \rightarrow SiO_5 + SiO_7$. The

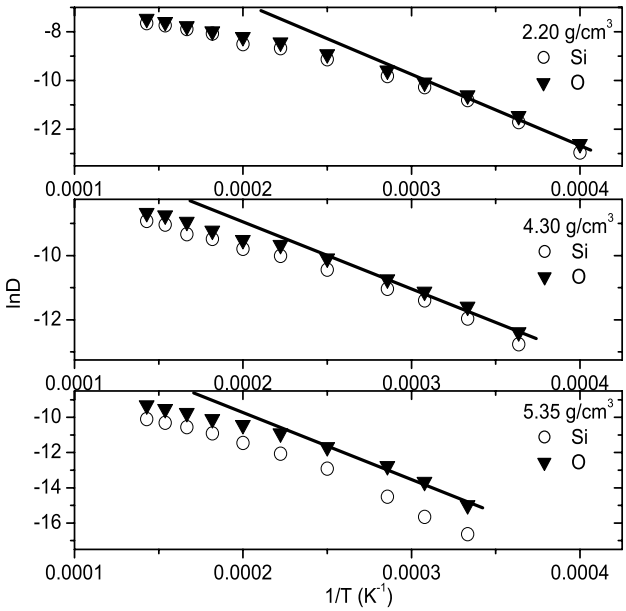

Figure 4. $1/T$ dependence of the logarithm of the diffusion constants of Si and O particles in liquid SiO_2. The straight lines just serve as guides for the eye.

Table 3. Number of Si atoms with corresponding coordination number Z_{Si-O} in 5.35 g cm^{-3} models at different temperatures.

	Z_{Si-O}				
T (K)	4	5	6	7	8
2500	7	146	690	154	3
3000	4	179	641	166	10
3250	12	191	621	167	9
3500	17	190	610	177	5
5000	24	225	556	181	14

higher the temperature, the higher the concentration of thermal defects, and indeed the same phenomenon is observed in table 3. The shooting up of the ratio $\frac{D_O}{D_{Si}}$ at around 3000 K may be related to the sudden changes in the oxygen diffusion mechanism caused by the melting of the 5.35 g cm^{-3} system (figure 3). The dominance of the non-connected diffusion of Si and O ions in high-density systems leads to an enhancement of the differences between their diffusion constants (see figure 4).

As mentioned in section 1, a power law behaviour for the dynamics in the network structure liquids has attracted great interest. However, the validity of the power law for diffusion at high pressure has been found only for water [5, 6] via both experiment and simulation. The question about the possible validity of a power law for the dynamics in other liquids under high pressure remains unresolved. In the present work, we aim to show the temperature dependence of the diffusion constant for models at three different densities, and indeed at high temperatures a deviation from an Arrhenius law was found (figure 4). After intensive testing we found that at $T \geqslant 4500$ K for the 2.20 g cm^{-3} models and at $T \geqslant 5000$ K for the 4.30 and 5.35 g cm^{-3}

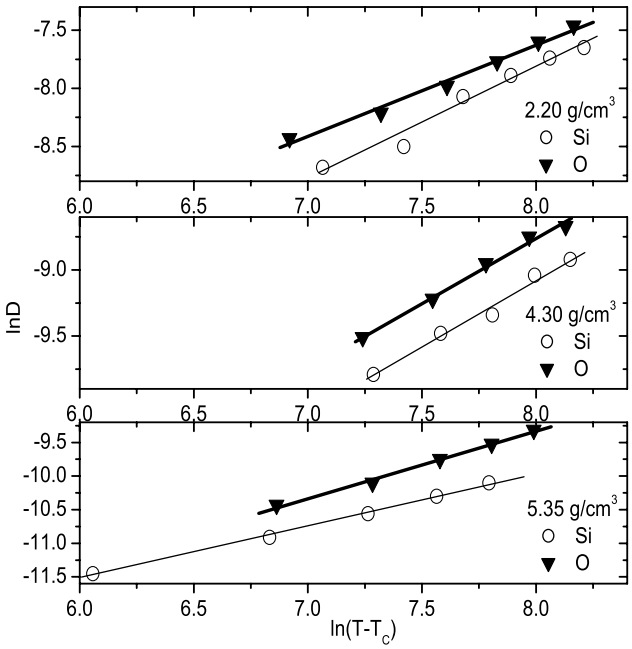

Figure 5. Fit of each isochore to the power law, $D \sim (T - T_c)^{\gamma}$, predicted by MCT.

Table 4. Parameters of power law, $D \sim (T - T_c)^{\gamma}$, and Arrhenius law, $D = D_0 \exp(-\frac{E}{k_B T})$, in liquid SiO_2 models at three different densities.

Density (g cm^{-3})	T_c (K)		γ		D_o (in 10^{-4} cm^2 s^{-1})		E (eV)	
	Si	O	Si	O	Si	O	Si	O
2.20	3330	3484	0.904	0.753	1589.763	1380.637	2.366	2.266
4.30	3538	3605	1.014	0.982	96.867	92.051	1.912	1.810
5.35	4573	4044	0.777	1.001	815.124	625.368	3.652	3.090

models, the temperature dependence of the diffusion constant shows a power law, as predicted by MCT: $D \sim (T - T_c)^{\gamma}$ (see figure 5). Also, at lower temperatures it shows an Arrhenius law: $D = D_0 \exp(-\frac{E}{k_B T})$. The parameters of these laws are presented in table 4. One can see that the exponent parameter γ increases with increasing pressure, like those observed experimentally for water [5] with the exception of the case of the Si particle at 5.35 g cm^{-3}. It is essential to notice that the parameter γ observed here for our silica is much less than that for water [5, 6]. Also, at the ambient pressure density of 2.20 g cm^{-3}, the parameter γ is at around values of 0.904 and 0.735 for both Si and O particles versus values of 2.15 and 2.05 for Si and O particles, obtained for BKS interatomic potential silica models at 2.37 g cm^{-3} [4]. Moreover, the MCT temperatures $T_c = 3330$ and 3484 K obtained at the density of 2.20 g cm^{-3} for Si and O are close to the value 3330 K in [4]. The discrepancy for γ may be related to the different interatomic potentials used in the simulations rather than to the difference in densities of the system. As noticed in [4], the dynamics quantities depend much more sensitively on the interatomic potentials than on the structural quantities.

Concerning the Arrhenius law, no systematic changes with pressure have been found (table 4). However, the activation energy for both Si and O particles is smaller than that

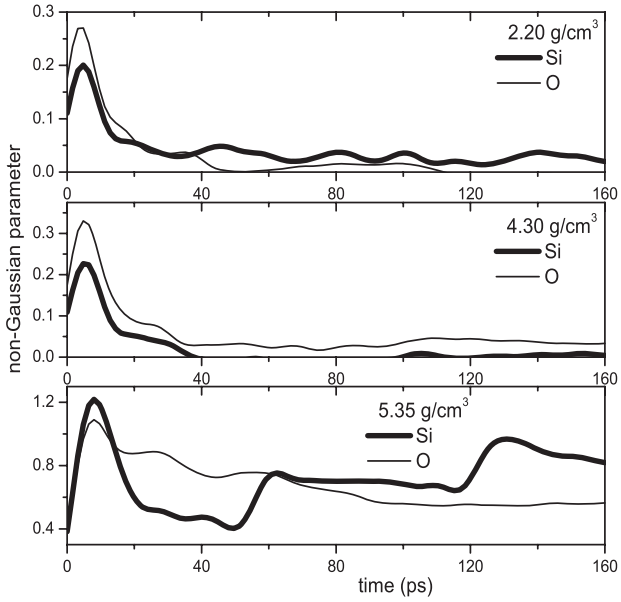

Figure 6. Non-Gaussian parameter in SiO_2 models obtained at 3000 K.

obtained experimentally for silica at ambient pressure, equal to 4.70 and 6 eV for oxygen and silicon, respectively [2, 3]. The discrepancy between our values for activation energy and experimental values may be related to the extremely high heating rate compared with those used in practice. On the other hand, although the adopted interatomic potentials with a Morse-type part for short-range interactions describe the structure and several thermodynamics properties of the vitreous silica well, they do not give the activation energy for diffusion in liquid silica accurately compared with that for BKS [4].

3.2. Dynamical heterogeneity

Dynamical heterogeneity (DH) in different supercooled systems at ambient pressure has been under intensive investigation in recent years (see [18–30] and references therein). In particular, DH in BKS interatomic potential silica models has been studied in detail [21–23]. However, no work related to DH in liquids under high pressure has been found in the literature. Also, it motivates us to carry out a study in heated silica models at different densities. The existence of DH in the system can be determined via the non-Gaussian parameter which has the form [18] $\alpha_2(t) = \frac{3\langle r^4(t)\rangle}{5\langle r^2(t)\rangle^2} - 1$. If the parameter $\alpha_2(t)$ differs from zero, it indicates the existence of DH in the system, which is clearly found for our liquid silica at 3000 K and at three different densities (figure 6). However, the DH in the models at the first two densities is much weaker than that at 5.35 g cm^{-3}, indicating the density dependence of DH in the system: the increase of DH with increasing density may be due to the enhancement of the cage effects. Moreover, one can see that the position of the first strong peak of the curves in figure 6 is nearly the same for the three different densities, and differs from each other just by the intensity of the peak. On the other hand, the occurrence of additional strong peaks in the non-Gaussian parameter curves at 5.35 g cm^{-3} has been found, unlike for the curves at lower densities. Non-smooth changes in the curves with time may be due to the statistics of the data in the present work being not very good. The DH in the system can be found directly via the atomic displacement

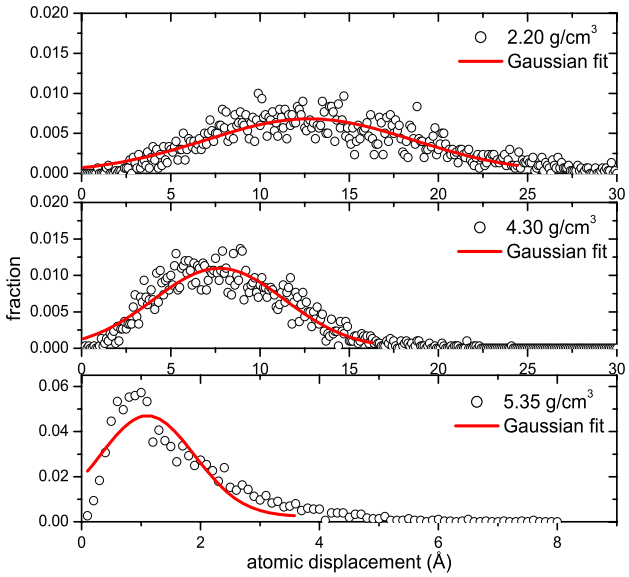

Figure 7. Atomic displacement distribution in SiO_2 models obtained at 3000 K by relaxing for 160 ps after heating.

(This figure is in colour only in the electronic version)

distribution (figure 7). In the homogenous system, such a distribution has a Gaussian form, and deviation from the Gaussian form due to a tail of the most mobile particles in the system serves as an indication of the existence of DH. Figure 7 shows that the deviation is more pronounced at 5.35 g cm^{-3} and is in good accordance with those observed via the non-Gaussian parameter. Also, one can approximately determine the fraction of the most mobile particles in the system via such a distribution, and it is equal to 4.40%, 2.83% and 6.83% (both Si and O particles together) for the models at 2.20, 4.30 and 5.35 g cm^{-3}, respectively (i.e. corresponding to the amount of atoms with displacement larger than 24.40, 16.00 and 3.60 Å for the models at 2.20, 4.30 and 5.35 g cm^{-3}, respectively). It is essential to notice that the fraction of the most mobile particles has been determined, and it is equal to 5% in Lennard-Jones and Dzugutov liquids [18, 28] or 6.5% in a glass-forming polymer melt [20]. For convenience, we take the fixed value of 5% for our silica at the three different densities. Many calculations show an important role of the most immobile particles in the DH of the system and, as shown in figure 7, the most immobile particles also make a significant contribution to the deviation of the atomic displacement distribution from the Gaussian form. Therefore, the dynamics of the 5% most immobile particles will be studied in detail here.

According to the results presented in figures 6 and 7, the DH in models at 2.20 and 4.30 g cm^{-3} is too weak, so we will focus our attention on the DH in models at 5.35 g cm^{-3}. In order to get more insight into the correlation between extremely low- or high-mobility particles in the system, we have calculated the cluster size distribution in the system at different densities. Also, like those observed in other liquids at ambient pressure, particles of extremely low or high mobility in models under high pressure also form clusters. However, the phenomenon is weak for models at 2.20 and 4.30 g cm^{-3} (not shown). At the higher density of 5.35 g cm^{-3}, we found that the number of particles in the largest cluster is 24 particles for the most mobile ones and, in contrast, 22 particles for the most immobile particles. These clusters are relatively small compared with those obtained in other liquids [18, 23], and this may be due to smaller

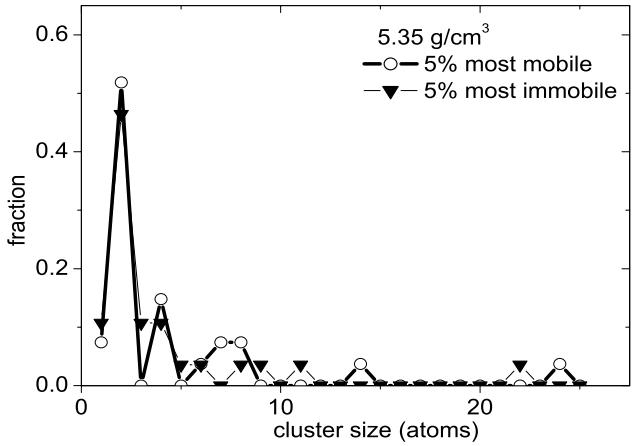

Figure 8. Cluster size distribution of the 5% most mobile or immobile particles in SiO_2 models obtained at 5.35 g cm^{-3} and at 3000 K by relaxing for 160 ps after heating.

model in the present work. However, it is close to those observed in a small Lennard-Jones system [26]. Also, such a cluster size distribution is similar for both the most mobile and immobile particles in the system, and it does not show a power law, unlike those observed for Lennard-Jones liquids [18], charged colloidal suspensions [19] or in Dzugutov liquid [28] (see figure 8). Possibly, it is caused by the different choices of interval time, Δt, for calculating the cluster size distribution. Commonly, Δt is chosen as the time when the non-Gaussian parameter $\alpha_2(t)$ or the mean cluster size is a maximum, and the corresponding cluster size distribution shows a power law, $P(n) \sim n^{-\gamma}$ (see [18, 19, 28]). The interval time Δt in the current work was chosen to be equal to 160 ps. The mean cluster size for both the most mobile and the immobile particles has a tendency to grow with density, and the mean cluster size of particles of extremely low or high mobility is nearly constant with temperature, with the exception of liquid at 5.35 g cm^{-3} (figure 9). For the model at 5.35 g cm^{-3}, the temperature dependence of the mean cluster of the 5% most mobile particles can be described approximately by an exponential decay, $S = S_0 + A \exp(-T/t_1)$ with the following parameters: $S_0 = 2.356$, $A = 570.995$ and $t_1 = 591.311$ (where S is the mean cluster size). In contrast, for the 5% most immobile particles in the system, it shows another law: the mean cluster size increases with increasing temperature and then decreases (figure 9). This indicates the different temperature dependence of the mean cluster size of the most mobile and immobile particles in the system. Likely, it was found that the temperature dependence of the mean cluster size of extremely fast particles in a cooled Lennard-Jones system [18] showed a power law, $S \sim (T - T_p)^{\gamma}$. Also, in contrast to what is found for the most mobile particles, the correlation between the most immobile particles does not show any singular behaviour. One can find that DH in 2.37 g cm^{-3} BKS interatomic potential silica models is more pronounced than in our models at 2.20 g cm^{-3} from the height of the non-Gaussian parameter, $\alpha_2(t)$, and from the strong correlation between the 5% most mobile particles in the system [23]. There are two possible reasons for the discrepancy. First, it is essential to notice that DH in several liquids mentioned above was mostly obtained by cooling from the melts, unlike those observed in the present work (i.e. obtained by heating from an amorphous state). Hoang showed that the dynamics including DH in models obtained by cooling from the melt and by heating from the amorphous phase is quite different due to

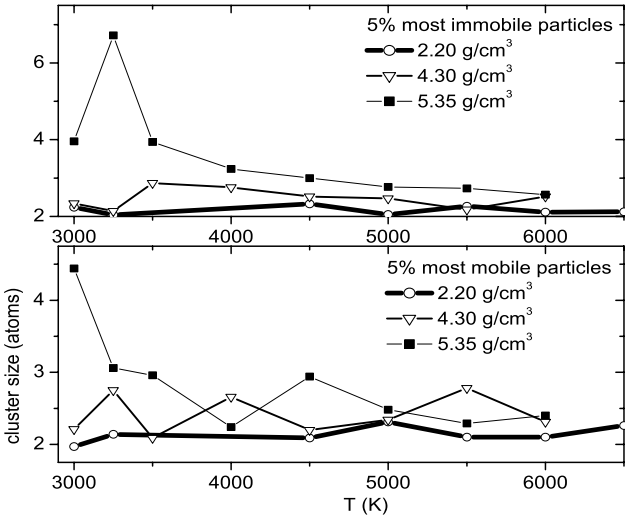

Figure 9. Temperature dependence of mean cluster size distribution in SiO_2 models obtained by relaxing for 160 ps after heating.

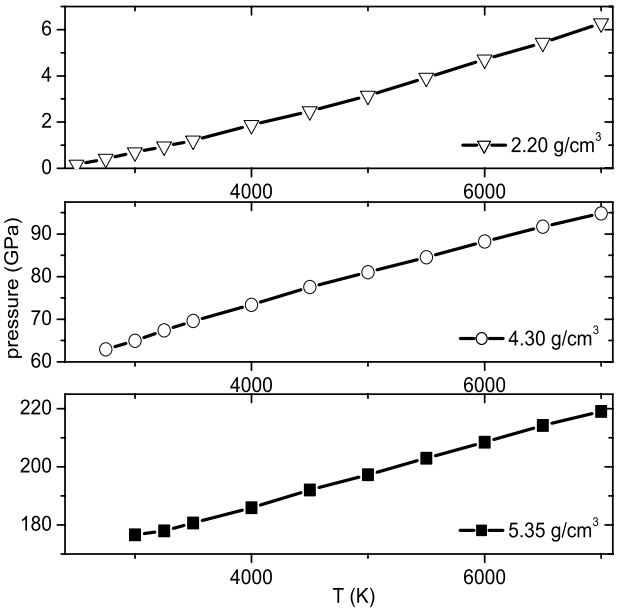

Figure 10. P–T diagram for in liquid SiO_2 at three different densities.

thermal hysteresis [30], and DH in the models obtained by cooling from the melts is much stronger than those in models obtained by heating from an amorphous state. The second reason is related to the different interatomic potentials used here and used in [23]. According to our recent calculations, DH in the same system depends strongly on the interatomic potentials used in the simulations [31].

Finally, we would like to stop here for discussion about the validity of the interatomic potentials used in our simulation at high pressures and temperatures. As presented in figure 10,

the pressure in the systems at 4.30 and 5.35 g cm^{-3} is rather high. The pressure dependence of the interatomic potentials is of great interest. However, it is too complex, and up to now the pressure changes of the interatomic potentials in the simulations have not been paid much attention. The fact is that simulation of SiO_2 at high density (i.e. high pressure) has been performed with fixed BKS or TTAM pair interatomic potentials [32–36]. The validity of the Morse-type potentials used in our simulations at high temperatures has been tested [14, 15]. However, their validity under high pressures has been under question. It is essential to notice that, by using these interatomic potentials, we found a pressure-induced phase transition from a tetrahedral to an octahedral network structure in amorphous silica, in accordance with those observed in practice [16]. Possibly, these interatomic potentials would not give the quantitative data for silica at very high pressures, but we are sure that they can give qualitative results. Moreover, silica is the most abundant substance in the earth, i.e. over 60% of the earth's crust is made of it and therefore its dynamics under high pressures and temperatures may be related to the flow of magma in the depth of the earth. This means that the study of the dynamics of silica under high pressure and temperatures is of great interest.

4. Conclusion

The main conclusions can be drawn:

(i) We found that the temperature dependence of the diffusion constant in simulated silica shows an Arrhenius law at temperatures above the melting point and shows a power law, $D \sim (T - T_C)^\gamma$, at higher temperatures for models at densities ranging from 2.20 to 5.35 g cm^{-3}. The exponent γ of a power law increases with pressure (or density), like those observed experimentally for water. This means that, upon heating the system from relatively low temperature to high temperature, we found a crossover from Arrhenian to non-Arrhenian dynamics in the liquids, i.e. corresponding to a transition from strong to fragile liquid behaviour in the system. Also, this is related to structural evolution in the system when the temperature increases [37]. It is essential to notice that diffusion under high pressures and temperatures in liquid silica with the BKS interatomic potentials has been studied and the reverse transition from fragile to strong liquid behaviour has been found upon cooling the system from high temperature towards the glass phase transition [32, 33]. However, the density range studied in [32, 33] is narrow, i.e. it ranged from 2.31 to 3.90 g cm^{-3}, and the validity of a power law for the dynamics in the system has not been tested yet.

(ii) We found the existence of dynamical heterogeneity in liquid silica models obtained by heating from an amorphous state under very high pressure (i.e. high density), and calculations show that this depends strongly on the density of the system, i.e. it increases with increasing density due to the enhancement of the cage effects.

(iii) Calculations show that the melting temperature of the system, T_m, depends strongly on the density, and that it increases with density.

Acknowledgments

This work was accomplished in the Computational Physics Lab of the College of Natural Sciences—National University of HochiMinh City (Vietnam).

References

[1] Woodcock L V, Angell C A and Cheeseman P 1976 *J. Chem. Phys.* **65** 1565
[2] Brebec G, Seguin R, Sella C, Bevenot J and Martin J C 1980 *Acta Metall.* **28** 327
[3] Mikkelsen J C 1984 *Appl. Phys. Lett.* **45** 1187
[4] Horbach J and Kob W 1999 *Phys. Rev.* B **60** 3169
[5] Prielmeier F X, Lang E W, Speedy R J and Ludemann H D 1987 *Phys. Rev. Lett.* **59** 1128
[6] Starr F W, Harrington S, Sciortino F and Stanley H E 1999 *Phys. Rev. Lett.* **82** 3629
[7] Starr F W, Harrington S, Sciortino F and Stanley H E 1999 *Phys. Rev.* E **60** 6757
[8] Hoang V V 2006 *J. Phys.: Condens. Matter* **18** 777
[9] Belashchenko D K 1997 *Russ. Chem. Rev.* **66** 733
[10] Tsuneyuki S, Tsukada M, Aoki H and Matsui Y 1988 *Phys. Rev. Lett.* **61** 869
[11] Tsuneyuki S and Matsui Y 1995 *Phys. Rev. Lett.* **74** 3197
[12] van Beest B W H, Kramer G J and van Santen R A 1990 *Phys. Rev. Lett.* **54** 1955
[13] Huang L, Duffrene L and Kieffer J 2004 *J. Non-Cryst. Solids* **349** 1
[14] Huff N T, Demiralp E, Cagin T and Goddard W A III 1999 *J. Non-Cryst. Solids* **253** 133
[15] Takada A, Richet P, Catlow C R A and Price G D 2004 *J. Non-Cryst. Solids* **345/346** 224
[16] Hoang V V, Hai N T and Zung H 2006 *Phys. Lett.* A **356** 246
[17] Lide D R (ed) 1996 *CRC Handbook of Chemistry and Physics* (NewYork: CRC Press)
[18] Donati C, Glotzer S C, Poole P H, Kob W and Plimpton S J 1999 *Phys. Rev.* E **60** 3107
[19] Tata B V R, Mohanty P S and Valsakumar M C 2002 *Phys. Rev. Lett.* **88** 018302
[20] Gebremichael Y, Schroder T B, Starr F W and Glotzer S C 2001 *Phys. Rev.* E **64** 051503
[21] Kerrache A, Teboul V, Guichaoua D and Monteil A 2003 *J. Non-Cryst. Solids* **322** 41
[22] Vogel M and Glotzer S C 2004 *Phys. Rev. Lett.* **92** 255901
[23] Vogel M and Glotzer S C 2004 *Phys. Rev.* E **70** 061504
[24] Hoang V V and Oh S K 2005 *J. Phys.: Condens. Matter* **17** 5179
[25] Hoang V V 2006 *Phys. Status Solidi* A **203** 478
[26] Vollmayr-Lee K, Kob W, Binder K and Zippelius A 2002 *J. Chem. Phys.* **116** 5158
[27] Hoang V V and Oh S K 2006 *Int. J. Mod. Phys.* B **20** 947
[28] Gebremichael Y, Vogel M and Glotzer S C 2004 *J. Chem. Phys.* **120** 4415
[29] Bedrov D, Smith G and Douglas J F 2004 *Polymer* **45** 3961
[30] Hoang V V 2005 *Eur. Phys. J.* B **48** 495
[31] Hoang V V 2006 *Eur. Phys. J.* B **54** 291
[32] Saika-Voivod I, Poole P H and Sciortino F 2001 *Nature* **412** 514
[33] Saika-Voivod I, Sciortino F and Poole P H 2004 *Phys. Rev.* E **69** 041503
[34] Shell M S, Debenedetti P G and Panagiotopoulos A Z 2002 *Phys. Rev.* B **66** 011202
[35] Tse J S and Klug D D 1992 *Phys. Rev.* B **46** 5933
[36] Rustad J R and Yuen D A 1990 *Phys. Rev.* A **42** 2081
[37] Saika-Voivod I, Sciortino F, Grande T and Poole P H 2004 *Phys. Rev.* E **70** 061507